Crystalline Symmetry-Protected Majorana Mode in Number-Conserving Dirac Semimetal Nanowires

Rui-Xing Zhang and Chao-Xing Liu

Phys. Rev. Lett. **120**, 156802 — Published 10 April 2018

DOI: 10.1103/PhysRevLett.120.156802

Crystalline symmetry protected Majorana mode in number-conserving Dirac semi-metal nanowires

Rui-Xing Zhang[1] and Chao-Xing Liu[1]

[1] *Department of Physics, The Pennsylvania State University, University Park, Pennsylvania 16802*

(Dated: March 2, 2018)

One of the cornerstones for topological quantum computations is Majorana zero mode, which has been intensively searched in fractional quantum Hall systems and topological superconductors. Several recent works suggest that such exotic mode can also exist in one dimensional (1D) interacting double-wire setup even without long-range superconductivity. A notable instability in these proposals comes from inter-channel single-particle tunneling that spoils the topological ground state degeneracy. Here we show that 1D Dirac semimetal (DSM) nanowire is an ideal number-conserving platform to realize such Majorana physics. By inserting magnetic flux, a DSM nanowire is driven into 1D crystalline-symmetry-protected semimetallic phase. Interaction enables the emergence of boundary Majorana zero modes, which is robust as a result of crystalline symmetry protection. We also explore several experimental consequences of Majorana signals.

Introduction - Anyons are natural generalizations of bosons and fermions from the perspective of quantum statistics. Interchanging a pair of anyons can induce either a non-trivial phase factor $e^{i\theta} \neq \pm 1$ in the wavefunction (Abelian anyons), or a rotation operation of the corresponding many-body wave function among a degenerate set of locally indistinguishable states (non-Abelian anyons) [1]. Anyonic physics was first pointed out in the context of fractional quantum Hall (FQH) effect [2], where anyons emerge as bulk quasiparticle excitations in an FQH system. A well-known example here is Majorana quasiparticle (Ising anyon), which emerges in a $\nu = \frac{5}{2}$ Moore-Read FQH state [3]. The non-Abelian statistics of Majorana quasiparticle makes it a promising candidate for building a topological quantum computer [4]. Besides FQH systems, Majorana physics was also studied in the topological superconductor (TSC) after the pioneering works by Read and Green [5], Ivanov [6] and Kitaev [7]. In particular, Kitaev pointed out the existence of boundary Majorana zero mode (MZM) in a one-dimensional (1D) p-wave TSC. Such TSC is topologically distinct from a conventional superconductor due to the MZM-induced ground state degeneracy (GSD) [8]. The degenerate ground states are further labeled by Z_2 fermion parity of the system, and their stability is guaranteed by this Z_2 parity symmetry. This Kitaev model serves as the underlying mechanism of recent intensive experimental efforts in realizing MZM physics in 1D semiconductor devices [9–14].

Theoretically, it was pointed out that MZM will become unstable in a single 1D quantum wire if strong quantum fluctuations destroy long-range superconductivity [15]. For a double-wire setup, however, MZMs can coexist with quantum fluctuations when inter-wire single-particle hopping vanishes while pair hopping interaction dominates [15–24]. Pair hopping process fluctuates particle number of each quantum wire only by a multiple of 2. Thus in each quantum wire, an emergent Z_2 fermion parity $P^{(2)}$ is well defined. Consequently, $P^{(2)}$ defines doubly degenerate ground states, which mimics the physics in Kitaev model. However, a well-known issue in the double-wire setup comes from "Z_2 parity breaking" induced by inter-wire single particle tunneling, which is generally unavoidable. Such tunneling process explicitly violates $P^{(2)}$ symmetry and thus spoils Majorana physics.

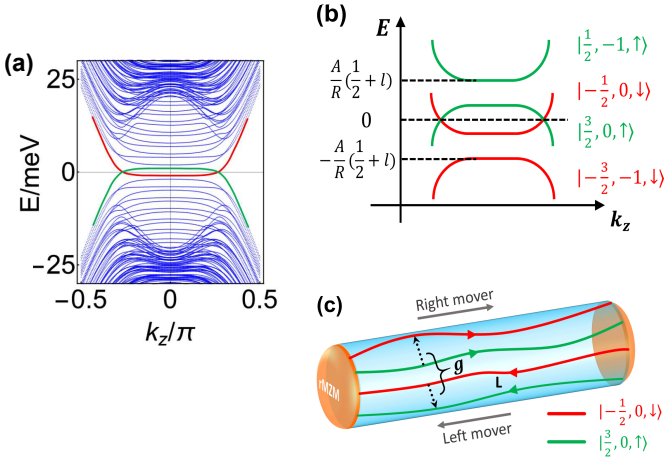

FIG. 1. In (a), DSM nanowire is driven into a rotation-symmetry-protected 1D semimetal when flux $\Phi = l\Phi_0$ ($\frac{1}{2} < l < \frac{3}{2}$) is inserted. The emerging 1D Dirac points originate from $|\frac{3}{2},0,\uparrow\rangle$ (green line) and $|-\frac{1}{2},0,\downarrow\rangle$ (red line), as shown in (b). In (c), we show the process of pair-hopping interaction g, where two "red" electrons hop to the "green" electron states simultaneously. This process respects four-fold rotation symmetry, and enables the emergence of Majorana end states.

In this work, we demonstrate how crystalline symmetries naturally solve the "$P^{(2)}$ breaking" issue, and thus stabilize the Majorana physics without long-range superconductivity. We show that 1D nanowire of three dimensional Dirac semimetals (DSM) [25, 26] possesses crystalline-symmetry-protected gapless Dirac points, offering us a material realization of stable semimetallic phase (Fig. 1 (a)). Therefore, a DSM nanowire man-

ifests itself as an effective double-wire setup, with each "quantum wire" labeled by a representation of the crystalline symmetry group. Inter-"wire" pair-hopping interaction drives the system into an interaction-enabled topological phase with doubly degenerate ground states and MZMs (Fig. 1 (c)). On the other hand, the origin of $P^{(2)}$-breaking, inter-"wire" *single*-particle tunneling, is forbidden in our rotation-invariant system, since it explicitly breaks the rotation symmetry. As a result, *rotational symmetry protects the robustness of the Majorana physics in the DSM nanowire system.* The boundary MZM in our setup bridges between ground states with different angular momentum representations of the rotational crystalline group. It is thus dubbed "representation MZM" (rMZM) to distinguish from conventional MZMs in TSCs. Experimentally, rMZM is shown to exhibit exponentially localized zero-bias peak signal, which can be detected via scanning tunneling microscopy (STM). We also propose a feasible setup to explore the transport physics of rMZM, where the transport phase diagram and experimental signals are discussed.

1D Dirac points in DSM nanowires - The following $k\cdot p$ Hamiltonian describes a typical DSM protected by the C_4 symmetry[25, 26]

$$H_{k\cdot p}=\begin{pmatrix} M(k) & Ak_- & 0 & 0\\ Ak_+ & -M(k) & 0 & 0\\ 0 & 0 & -M(k) & -Ak_-\\ 0 & 0 & -Ak_+ & M(k)\end{pmatrix}, \quad (1)$$

The basis function Ψ is $(|P,\frac{3}{2}\rangle,|S,\frac{1}{2}\rangle,|S,-\frac{1}{2}\rangle,|P,-\frac{3}{2}\rangle)^T$, where spin-orbit-coupled angular momentum $J\in\{\pm\frac{1}{2},\pm\frac{3}{2}\}$ acts as a pseudo-spin index. Notice that $H_{k\cdot p}$ takes a block-diagonal form of $\mathrm{diag}(H_\uparrow,H_\downarrow)$, with each block describing a Weyl Hamiltonian in the corresponding spin ($\uparrow$ or $\downarrow$) sector. Here $M(k)=M_0-M_1k_z^2-M_2(k_x^2+k_y^2)$ and $k_\pm=k_x\pm ik_y$, with $A>0$ and $M_{0,1,2}>0$. The bulk Dirac points are aligned along rotational invariant k_z axis at $k_z=\pm\sqrt{M_0/M_1}$. The $\uparrow$ and $\downarrow$ sectors are related via $H_\downarrow(M(k),A)=H_\uparrow(-M(k),-A)$. Thus, we will focus on $H_\uparrow$, and the properties of $H_\downarrow$ can be obtained analogously.

The DSM nanowire can be better described in cylindrical coordinates. We rewrite $H_\uparrow$ in terms of $k_r=-i\partial_r$ and $k_\theta=-\frac{i}{r}\partial_\theta$ with angular variables $r=\sqrt{x^2+y^2}$ and $\theta=\arctan\frac{y}{x}$. Solving the eigen-state problem [27], the low-energy eigenstates of $H_\uparrow$ are found to be Fermi arc states on the side surface of the nanowire [28]. For a nanowire with radius R, surface Fermi arc spectrum $E_\uparrow=-\frac{A}{R}(m+\frac{1}{2})$, where $m=0,\pm1,\pm2,...$ is the eigenvalue of k_θ. The spin-down part of H_0 behaves similarly with $E_\downarrow=\frac{A}{R}(m+\frac{1}{2})$. Notice that the complete Fermi arc spectrum always exhibits a finite gap of A/R, which originates from the π spin Berry phase of the Fermi arc states [29]. In this nanowire geometry, total angular momentum J_{tot} is a good quantum number, while it is actually composed of two parts: (1) angular contribution from k_θ and (2) pseudo-spin J which is encoded in the basis Ψ. In particular, we find that a state with $k_\theta=m$ carries $J_{tot}=m+2\sigma+\frac{1}{2}$ in the spin-σ ($\sigma=\pm\frac{1}{2}$) sector. Thus, we label an energy eigen-state as $|J_{tot},m,\sigma\rangle$ where spin index $\sigma\in\{\uparrow,\downarrow\}$.

The 1D Dirac points can be realized by inserting magnetic flux to remove the Berry phase effect. The applied magnetic field should be precisely aligned along the nanowire to preserve the C_4 symmetry. With flux $\Phi=l$ (in units of $\Phi_0=h/e$) inserted, $E_{\uparrow/\downarrow}=\mp\frac{A}{R}(m+\frac{1}{2}-l)$. The π Berry phase is exactly canceled, when π-flux ($l=\frac{1}{2}$) is inserted. Consequently, $|\frac{3}{2},0,\uparrow\rangle$ touches $|-\frac{1}{2},0,\downarrow\rangle$ at $k_z=0$, which is similar to the worm-hole effect of topological insulator nanowire [30]. When Φ is further increased, $|\frac{3}{2},0,\uparrow\rangle$ intersects with $|-\frac{1}{2},0,\downarrow\rangle$ to form a gapless inverted band structure (1D Dirac points), as shown in Fig. 1 (b). Since $|\frac{3}{2},0,\uparrow\rangle$ and $|-\frac{1}{2},0,\downarrow\rangle$ belong to different representations of the rotational group, the 1D Dirac points are robust and thus protected by C_4 symmetry. In Fig. 1 (a), we verify the above results in the tight-binding model obtained from regularizing the $k\cdot p$ Hamiltonian on a cubic lattice [31]. The magnetic field required for inducing 2π flux is around 1T for a nanowire with a diameter of 100 nm [27]. This is how we assemble a 1D rotation-symmetry-protected semimetal by inserting magnetic flux into the DSM nanowire.

Interaction-induced Majorana physics - The low-energy theory of 1D Dirac points is well captured by the 2-channel Luttinger liquid (LL) theory,

$$H_0=\sum_{s=1,2}\int dx\frac{v}{2}[\psi^\dagger_{s,R}(x)\partial_x\psi_{s,R}(x)-\psi^\dagger_{s,L}(x)\partial_x\psi_{s,L}(x)].$$

Here $\psi^\dagger_{1,R(L)}$ creates a right (left) moving electron with $J_{tot}=-\frac{1}{2}$, while $\psi^\dagger_{2,R(L)}$ creates a right (left) moving electron with $J_{tot}=\frac{3}{2}$. Two-particle processes that preserve both $U(1)$ charge conservation and C_4 rotation symmetry [32] are:

$$\begin{aligned}H_1=\int dx[&g\psi^\dagger_{1,R}\psi^\dagger_{1,L}\psi_{2,R}\psi_{2,L}+g_1\psi^\dagger_{1,R}\psi^\dagger_{2,L}\psi_{2,R}\psi_{1,L}\\&+g_2\psi^\dagger_{1,R}\psi^\dagger_{2,R}\psi_{2,L}\psi_{1,L}+h.c.]\end{aligned} \quad (2)$$

If we move the Fermi level slightly away from the Dirac points (zero energy in Fig. 1 (a) and (b)), both g_1 and g_2 scatterings involve certain amount of momentum transfer, and will be suppressed in a translational invariant system. Inter-channel pair-hopping g, however, preserves both momentum conservation and C_4 symmetry (angular momentum transfer $\Delta J_{tot}=4$). As will be shown below, it is g that is responsible for Majorana physics.

We next apply Abelian bosonization technique [33] and define $\psi_{s,R}\sim e^{i\sqrt{\pi}(\phi_s-\theta_s)}$ and $\psi_{s,L}\sim e^{-i\sqrt{\pi}(\phi_s+\theta_s)}$ following the convention in [34]. It is convenient to introduce the bonding and anti-bonding fields as $\phi_\pm=$

$\frac{1}{\sqrt{2}}(\phi_1 \pm \phi_2)$ and $\theta_\pm = \frac{1}{\sqrt{2}}(\theta_1 \pm \theta_2)$, as well as $K_\pm$ to be the Luttinger parameters for bonding and anti-bonding channel. The bonding sector remains gapless, while the anti-bonding sector might open up a non-trivial gap with the Hamiltonian

$$H_- = \int dx \frac{v}{2}[K_-(\partial_x\phi_-)^2 + \frac{1}{K_-}(\partial_x\theta_-)^2] + g\int dx \cos 2\sqrt{2\pi}\theta_-. \quad (3)$$

We will focus on $K_- < 1$ where g is relevant under renormalization group analysis. At Luther-Emery point ($K_- = \frac{1}{2}$), Eq. 3 can be exactly mapped to the topological Kitaev model with MZM end states [16, 27]. Such mapping is achieved by refermionizing Eq. 3 with $\tilde{\psi}_R \sim e^{i\sqrt{\pi}(\tilde{\phi}-\tilde{\theta})}$ and $\tilde{\psi}_L \sim e^{-i\sqrt{\pi}(\tilde{\phi}+\tilde{\theta})}$, where $\tilde{\phi} = \phi_-/\sqrt{2}$ and $\tilde{\theta} = \sqrt{2}\theta_-$. Away from $K_- = \frac{1}{2}$, the above mapping fails while we will show that Majorana physics (both GSD and Majorana end states) persists.

The ground state is obtained by minimizing $\cos 2\sqrt{2\pi}\theta_-$ and pinning $\theta_- = (n_\theta + \frac{1}{2})\sqrt{\pi/2}$, where $n_\theta \in \mathbb{Z}$ is an integer-valued operator. Since θ_- has $\sqrt{2\pi}$ periodicity, there are two degenerate ground states $|\theta_- = \pm\frac{1}{2}\sqrt{\frac{\pi}{2}}\rangle$, which are characterized by the emergent Z_2 fermion parity $P^{(2)}$. Physically, $P^{(2)}$ counts the parity of electron number in the $J_{tot} = -\frac{1}{2}$ subspace,

$$P^{(2)} = (-1)^{\sqrt{\frac{1}{\pi}}\int_0^L dx\partial_x\phi_1} = P_+P_-, \quad (4)$$

where a nanowire with finite length L is considered and $P_\pm = e^{i\sqrt{\pi/2}(\phi_\pm(L)-\phi_\pm(0))}$. With $P^{(2)}\theta_-(P^{(2)})^{-1} = \theta_- - \sqrt{\frac{\pi}{2}}$, $P^{(2)}$ interchanges $|\theta_- = \pm\frac{1}{2}\sqrt{\frac{\pi}{2}}\rangle$ from one to another. Quantum superposition principle, however, allows us to define the following degenerate ground states,

$$|\pm\rangle = \frac{1}{\sqrt{2}}[|\theta_- = \frac{1}{2}\sqrt{\frac{\pi}{2}}\rangle \pm |\theta_- = -\frac{1}{2}\sqrt{\frac{\pi}{2}}\rangle], \quad (5)$$

where $|+\rangle$ and $|-\rangle$ are characterized by even and odd $P^{(2)}$ parity, respectively. Since $P^{(2)}$ is a global property of the system, the degeneracy here is topological, which can NOT be distinguished via any local measurement.

Topological GSD can also be revealed by constructing rMZM operators explicitly. Imposing open boundary condition at $x = 0$ gives rise to $\psi_{l,L}(0) + \psi_{l,R}(0) = 0$ for $l = 1, 2$, which corresponds to $\phi_l(0) = n_l^{(1)}\sqrt{\pi}$ up to an unimportant constant. Here, $n_l^{(1)} \in \mathbb{Z}$ is an integer-valued operator. Introducing $n_+^{(1)} = n_1^{(1)} + n_2^{(1)}$ and $n_-^{(1)} = n_1^{(1)}$, the boundary condition fixes the value of $\phi_\pm$ as $\phi_+(0) = n_+^{(1)}\sqrt{\pi/2}$ and $\phi_-(0) = (2n_-^{(1)} - n_+^{(1)})\sqrt{\pi/2}$. It is important to notice that $[n_-^{(1)}(x), n_\theta(x')] = \frac{i}{\pi}\Theta(x - x')$, while $n_+^{(1)}$ always commutes with n_θ and behaves like a c-number. Following Ref. [35], we construct rMZM operator α_1 at $x = 0$ and α_2 at $x = L$ as,

$$\alpha_1 = e^{i\pi(n_-^{(1)}+n_\theta)}, \quad (6)$$

$$\alpha_2 = e^{i\pi(n_-^{(2)}+n_\theta)}, \quad (7)$$

where we have defined the boundary condition at $x = L$ to be $\phi_+(L) = n_+^{(2)}\sqrt{\pi/2}$ and $\phi_-(L) = (2n_-^{(2)} - n_+^{(2)})\sqrt{\pi/2}$ in a similar way. The Majorana properties of $\alpha_{1,2}$ can be easily checked, where $[\alpha_{1,2}, H_-] = 0$ and $\alpha_1^2 = \alpha_2^2 = 1$. Starting from a ground state $|+\rangle$, one can easily show that $\alpha_{1,2}|+\rangle = |-\rangle$ up to some phase factors. This also proves the topological GSD.

The essential role of C_4 symmetry in protecting rMZM should be emphasized. C_4 symmetry enforces inter-channel single-particle tunneling events to vanish as they break C_4 explicitly, which makes $P^{(2)}$ symmetry well-defined. Since $C_4\theta_-C_4^{-1} = \theta_- + \sqrt{\frac{\pi}{2}}$, it is easy to check that $C_4|\pm\rangle = \pm|\pm\rangle$, which proves $C_4 = P^{(2)}$. The equivalence between a N-fold discrete symmetry Z_N and an emergent Z_M fermion parity $P^{(M)}$ is a quite general result for two-channel systems, which is discussed in details in the supplementary materials [27].

We stress that our theory is not limited to the C_4-symmetric DSM nanowire. For a 1D nanowire growing along the x direction, the crystalline structure in the cross-section (y-z plane) is characterized by a two-dimensional (2D) point group G_{2D}, where every symmetry operation in G_{2D} leaves the x direction invariant. Therefore, it is natural to generalize our theory from C_4 group to general 2D point groups. In [27], we identify simple criteria to determine whether a given symmetry group G could give rise to $P^{(2)}$ parity and present a complete discussion of all 2D point groups, as well as their double groups. In particular, our theory predicts all possible irreducible representations for each G_{2D} that could support Majorana physics, and thus establishes the guideline for the search of other candidate materials.

Experimental detection - One important approach to probe Majorana signals is to map out the spatial profile of spectral density using STM technique, and seek for exponentially localized zero-bias peak that originates from MZM bound state. Following this logic, we consider the single-electron-tunneling problem from a Fermi liquid lead to the DSM nanowire and seek for rMZM signals. This tunneling process changes both electron number and $P^{(2)}$ simultaneously. In particular, the ground state is changed from $|0\rangle = |N, p\rangle$ with N electrons and $P^{(2)} = p$ to $|1\rangle = |N + 1, -p\rangle$ with $N + 1$ electrons and $P^{(2)} = -p$ via this tunneling process. For a DSM nanowire at $x \in [0, L]$, in the $L \to \infty$ limit, transition matrix element of injecting a single electron at $x = x_0$ ($0 \le x_0 \ll L$) can be calculated with the help of mode expansion technique [27, 36], and the resulting spectral density is

$$\rho(x, \omega \to 0) = |\langle 1|\psi_{1,R}^\dagger|0\rangle|^2 = \mathcal{N}(x, \epsilon, K_\pm)\, e^{-\frac{\pi}{4K_-}\frac{x}{\xi}} \quad (8)$$

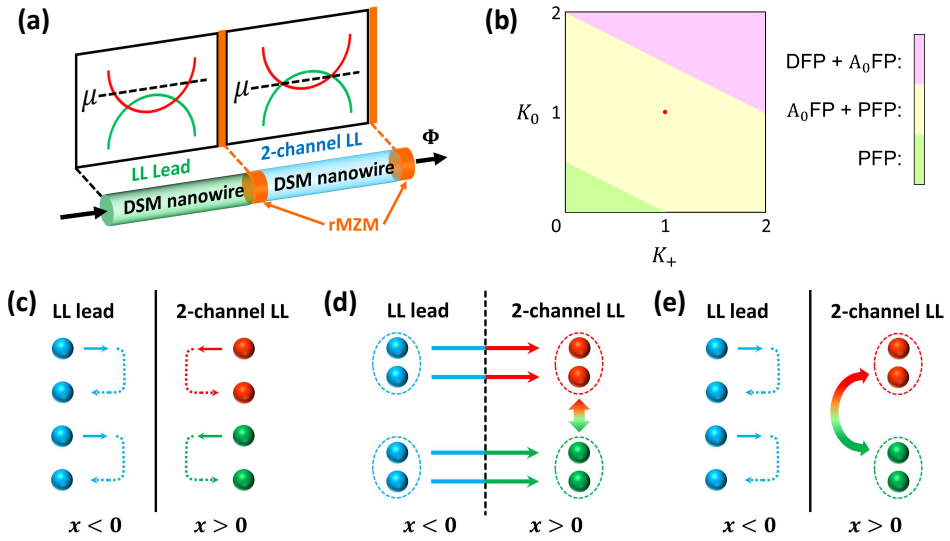

FIG. 2. (a) We apply a step-function gate to DSM nanowire to fabricate the 2LL/LL configuration. (b) Tunneling phase diagram of 2LL/LL junction with $K_- < 1$. In (c) - (e), we systematically plot the boundary conditions of the following fixed points: DFP, PFP and A_0FP. The dashed circle that contains a pair of electrons signals pair-tunneling/backscattering process.

where $\xi = \sqrt{\frac{v}{8\pi g K_-}}$ is the correlation length of the system and ϵ is the short distance cut-off. While $\mathcal{N}(x, \epsilon, K_\pm)$ counts the power-law contribution of this transition process [27], the exponential part of $\rho(x, \omega \to 0)$ unambiguously reveals an exponentially localized rMZM on the boundary, which is ready to be detected using STM technique. Since $\xi \sim 1/\sqrt{gK_-}$, the stronger the interaction, the more localized rMZM will be.

Finally, we consider a 2-channel LL/LL lead (2LL/LL) junction, which can be experimentally achieved by applying a step-function-like gating to the DSM nanowire, as shown in Fig. 2 (a). With this gating configuration, the right part of the nanowire ($x > 0$) is in the 2-channel LL regime, while the left part ($x < 0$) becomes a single-channel LL that plays the role of a lead. The rMZM is expected at the interface between 2-channel LL and single-channel LL ($x = 0$).

The transport physics of 2LL/LL junction is characterized by tunneling fixed points. Fig. 2 (c) - (e) depict three stable fixed points for different physical boundary conditions at the interface. (i) Disconnecting fixed point (DFP) signals the promotion of normal reflection process, where electrons will be perfectly reflected at the interface between 2LL and LL (Fig. 2 (c)). (ii) Pair-tunneling fixed point (PFP) characterizes the resonant Andreev reflection process [37], where electrons will pair up and tunnel through the interface without any backscattering, as shown in Fig. 2 (d). (iii) A_0 fixed point (A_0FP) also signals normal reflection process of electrons from the LL lead, while on the 2LL side, electrons of channel-1 (channel-2) will pair up and be scattered together into channel-2 (channel-1) at the interface, as shown in Fig. 2 (e). This is essentially different from the case of DFP, where electrons will be individually backscattered without any channel-switching. We notice that DFP and PFP have been previously discussed in a TSC/LL junction [38], while A_0FP is a new fixed point in our system.

With the "delayed evaluation of boundary condition" (DEBC) method [39, 40], we verified the existence of all three fixed points (DFP, PFP, and A_0FP) and evaluate the scaling dimensions of perturbation terms at each fixed point. A brief introduction of this method and details of fixed point information can be found in the supplementary materials [27]. The complete phase diagram is mapped out in Fig. 2 (b) for $K_- < 1$. In the strongly attractive regime ($K_+ < 1 - 2K_0$), PFP is stable and promotes the Andreev reflection process. In the strongly repulsive limit ($K_+ > 4 - 2K_0$), both DFP and A_0FP are stable, and the tunneling conductance is suppressed.

A realistic system is most likely to fall into the weakly interacting regime ($K_0, K_+ \approx 1$) with both stable PFP and A_0FP. In a transport measurement, one expects a zero-bias conductance peak at PFP, while a vanishing conductance at A_0FP. The co-existence of two stable fixed points suggests the emergence of an intermediate unstable fixed point which characterizes the transition between PFP and A_0FP. This novel phase transition is intriguing, which is definitely worthy to be explored in future works. At last, the role of rMZM is explored by mapping out a Majorana-free phase diagram where we quench pair-hopping interaction g at $x > 0$. In this case, we find a completely different phase diagram with more exotic phases [27]. Especially, the system falls into A_0FP near $K_{0,+} \approx 1$, while PFP only shows up in the strongly attractive regime. Therefore, the appearance of weakly interacting PFP in Fig. 2 (b) is a direct consequence of

rMZM, and serves as a transport evidence of rMZM.

Discussion - In summary, we have proposed that magnetic-flux insertion drives DSM nanowire into a 1D crystalline-symmetry-protected semimetal, which serves as an ideal platform to realize Majorana physics without long-range superconductivity. In particular, crystalline symmetry forbids inter-channel single-particle tunneling, and thus guarantees the stability of Majorana physics. We notice that DSM nanowire of Cd_3As_2 has been successfully fabricated [41, 42], while these nanowires have been grown along [112] direction, so that C_4 rotation symmetry is explicitly broken and fails to support rMZM. Other promising candidate materials include heterostructures of Kondo materials [43], where a correlated DSM phase protected by C_4 symmetry is found. Finally, we emphasize once again that our theory is general and not limited to the DSM nanowires. The classification of 2D point groups in the supplementary materials will inspire more future efforts into realizing symmetry-protected Majoranas in number conserving systems.

Acknowledgement - The authors are indebted to Meng Cheng for valuable suggestions. R.-X.Z would like to thank Jian-Xiao Zhang, Jiabin Yu and Jiahua Gu for helpful discussions, and particularly Lun-Hui Hu for collaboration on a closely related project. C.-X. L. and R.-X.Z acknowledge support from Office of Naval Research (Grant No. N00014-15-1-2675).

[1] C. Nayak, S. H. Simon, A. Stern, M. Freedman, and S. D. Sarma, Reviews of Modern Physics **80**, 1083 (2008).
[2] D. C. Tsui, H. L. Stormer, and A. C. Gossard, Physical Review Letters **48**, 1559 (1982).
[3] G. Moore and N. Read, Nuclear Physics B **360**, 362 (1991).
[4] A. Y. Kitaev, Annals of Physics **303**, 2 (2003).
[5] N. Read and D. Green, Physical Review B **61**, 10267 (2000).
[6] D. A. Ivanov, Physical Review Letters **86**, 268 (2001).
[7] A. Y. Kitaev, Physics-Uspekhi **44**, 131 (2001).
[8] J. Alicea, Reports on Progress in Physics **75**, 076501 (2012).
[9] R. M. Lutchyn, J. D. Sau, and S. D. Sarma, Physical review letters **105**, 077001 (2010).
[10] Y. Oreg, G. Refael, and F. von Oppen, Physical review letters **105**, 177002 (2010).
[11] V. Mourik, K. Zuo, S. M. Frolov, S. Plissard, E. Bakkers, and L. P. Kouwenhoven, Science **336**, 1003 (2012).
[12] A. Das, Y. Ronen, Y. Most, Y. Oreg, M. Heiblum, and H. Shtrikman, Nature Physics **8**, 887 (2012).
[13] S. Nadj-Perge, I. K. Drozdov, J. Li, H. Chen, S. Jeon, J. Seo, A. H. MacDonald, B. A. Bernevig, and A. Yazdani, Science **346**, 602 (2014).
[14] H. Zhang, C.-X. Liu, S. Gazibegovic, D. Xu, J. A. Logan, G. Wang, N. van Loo, J. D. Bommer, M. W. de Moor, D. Car, et al., arXiv preprint arXiv:1710.10701 (2017).
[15] L. Fidkowski, R. M. Lutchyn, C. Nayak, and M. P. Fisher, Physical Review B **84**, 195436 (2011).
[16] M. Cheng and H.-H. Tu, Physical Review B **84**, 094503 (2011).
[17] J. D. Sau, B. Halperin, K. Flensberg, and S. D. Sarma, Physical Review B **84**, 144509 (2011).
[18] C. V. Kraus, M. Dalmonte, M. A. Baranov, A. M. Läuchli, and P. Zoller, Physical review letters **111**, 173004 (2013).
[19] G. Ortiz, J. Dukelsky, E. Cobanera, C. Esebbag, and C. Beenakker, Physical review letters **113**, 267002 (2014).
[20] J. Klinovaja and D. Loss, Physical review letters **112**, 246403 (2014).
[21] F. Iemini, L. Mazza, D. Rossini, R. Fazio, and S. Diehl, Physical review letters **115**, 156402 (2015).
[22] N. Lang and H. P. Büchler, Physical Review B **92**, 041118 (2015).
[23] C. Chen, W. Yan, C. Ting, Y. Chen, and F. Burnell, arXiv preprint arXiv:1701.01794 (2017).
[24] F. Iemini, L. Mazza, L. Fallani, P. Zoller, R. Fazio, and M. Dalmonte, Physical Review Letters **118**, 200404 (2017).
[25] Z. Wang, Y. Sun, X.-Q. Chen, C. Franchini, G. Xu, H. Weng, X. Dai, and Z. Fang, Physical Review B **85**, 195320 (2012).
[26] Z. Wang, H. Weng, Q. Wu, X. Dai, and Z. Fang, Physical Review B **88**, 125427 (2013).
[27] See Supplementary Materials at XX for a solution of Dirac semimetal in cylindrical coordinates, the magnetic field dependence, a microscopic derivation of pair-hopping interaction g, an estimation of the magnitude of g, a discussion about Klein factors and the Majorana solution at Luther-Emery point, a discussion of the emergent Z_M fermion parity from a Z_N symmetry, a generalization from C_4 symmetry to the 2D point groups, a detailed calculation of single electron tunneling amplitude, an introduction of DEBC method and a detailed discussion about the 2LL/LL junction phase diagram, which contains [44–53].
[28] K.-I. Imura and Y. Takane, Physical Review B **84**, 245415 (2011).
[29] In the limit $R \to \infty$, the energy gap in both spin sectors approaches zero and DSM nanowire evolves into a bulk DSM sample with two bulk Dirac points connected by Fermi arc states.
[30] G. Rosenberg, H.-M. Guo, and M. Franz, Physical Review B **82**, 041104 (2010).
[31] The nanowire configuration is modeled by taking periodic (open) boundary condition along the z (x and y) direction. Realistic parameters of Cd_2As_3 are applied in the calculation, and the cross section in the x-y plane is chosen to be a 16×16 square.
[32] Notice that the effective $k \cdot p$ Hamiltonian in Eq. 1 has the full-rotation $O(2)$ symmetry, since we focused on the continuum limit and dropped higher order terms. However, when we consider interaction effects, it is important to distinguish this artificial $O(2)$ symmetry from the realistic C_4 symmetry. This is because O(2) is a stronger symmetry and also imposes a stronger constraint to interaction terms. In particular, the pair-hopping term g that leads to Majorana physics transfers angular momentum by $\Delta J_{tot} = 4$. As a result, pair-hopping interaction only preserves C_4 symmetry, but explicitly breaks O(2) symmetry.
[33] T. Giamarchi, Quantum physics in one dimension, Vol. 121 (Oxford university press, 2004).

[34] E. Fradkin, Field theories of condensed matter physics (Cambridge University Press, 2013).
[35] D. J. Clarke, J. Alicea, and K. Shtengel, Nature Communications **4**, 1348 (2013).
[36] A. Keselman and E. Berg, Physical Review B **91**, 235309 (2015).
[37] K. T. Law, P. A. Lee, and T. K. Ng, Physical review letters **103**, 237001 (2009).
[38] L. Fidkowski, J. Alicea, N. H. Lindner, R. M. Lutchyn, and M. P. Fisher, Physical Review B **85**, 245121 (2012).
[39] M. Oshikawa, C. Chamon, and I. Affleck, Journal of Statistical Mechanics: Theory and Experiment **2006**, P02008 (2006).
[40] C.-Y. Hou, A. Rahmani, A. E. Feiguin, and C. Chamon, Physical Review B **86**, 075451 (2012).
[41] C.-Z. Li, L.-X. Wang, H. Liu, J. Wang, Z.-M. Liao, and D.-P. Yu, Nature communications **6** (2015).
[42] L.-X. Wang, C.-Z. Li, D.-P. Yu, and Z.-M. Liao, Nature communications **7** (2016).
[43] S. Ok, M. Legner, T. Neupert, and A. M. Cook, arXiv preprint arXiv:1703.03804 (2017).
[44] C. Kane, R. Mukhopadhyay, and T. Lubensky, Physical review letters **88**, 036401 (2002).
[45] J. C. Teo and C. Kane, Physical Review B **89**, 085101 (2014).
[46] T. Neupert, C. Chamon, C. Mudry, and R. Thomale, Physical Review B **90**, 205101 (2014).
[47] E. Sagi and Y. Oreg, Physical Review B **90**, 201102 (2014).
[48] J. Klinovaja and Y. Tserkovnyak, Physical Review B **90**, 115426 (2014).
[49] B. Bellazzini, M. Mintchev, and P. Sorba, Journal of Physics A: Mathematical and Theoretical **40**, 2485 (2007).
[50] B. Bellazzini, M. Burrello, M. Mintchev, and P. Sorba, arXiv preprint arXiv:0801.2852 (2008).
[51] B. Bellazzini, M. Mintchev, and P. Sorba, Physical Review B **80**, 245441 (2009).
[52] A. Agarwal, S. Das, S. Rao, and D. Sen, Physical review letters **103**, 026401 (2009).
[53] J.-P. Jay-Gerin, M. Aubin, and L. Caron, Solid State Communications **21**, 771 (1977).